analytical chemistry

Article

pubs.acs.org/ac

Label-Free Surface-Enhanced Raman Spectroscopy for Sensitive DNA Detection by DNA-Mediated Silver Nanoparticle Growth

Fenglei Gao, Jianping Lei, and Huangxian Ju*

State Key Laboratory of Analytical Chemistry for Life Science, School of Chemistry and Chemical Engineering, Nanjing University, Nanjing 210093, P. R. China

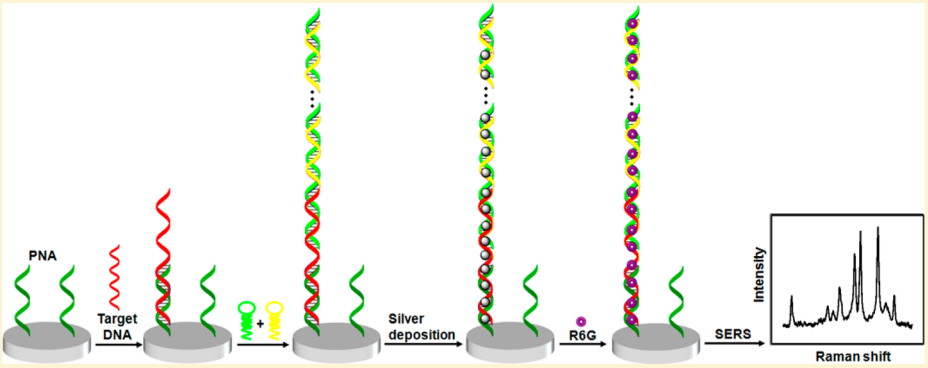

ABSTRACT: This work designed a label-free strategy for surface-enhanced Raman spectroscopic (SERS) detection of target DNA on a peptide nucleic acid (PNA) modified glass slide. Upon hybridization of the PNA with target DNA, the surface became negatively charged and allowed the absorption of silver ions on the DNA skeleton. After chemical reduction by hydroquinone, the formed silver nanoparticles could be further grown with a silver enhancement step to amplify the detectable SERS signal by absorbing rhodamine 6G as a SERS reporter on a silver nanoparticle surface. The growth of silver nanoparticles was characterized with X-ray photoelectron spectroscopy and a scanning electron microscopic image. The label-free SERS method achieved the detection of DNA with a linear range from 1.0×10^{-10} to 1.0×10^{-6} M and a detection limit of 45 pM. Through introducing a hybridization chain reaction to increase the DNA length, the Raman signal was further amplified, leading to a detection limit of 3.4 pM. This approach could discriminate perfectly matched target DNA from single-base mismatch DNA. This strategy possessed good capacity to integrate other amplification techniques for sensitive, high-throughput detection of genes.

Surface-enhanced Raman spectroscopy (SERS) as a significant technique has garnered considerable attention because of its single-molecule sensitivity, molecular specificity, and insensitivity to quenching.[1−5] These distinct advantages have led to the development of a number of ingenious SERS strategies for DNA detection. These strategies can be divided into three categories: sandwich hybridization of target DNA with capture and SERS reporter labeled sequences,[6−8] target DNA-triggered assembly of DNA nanostructures with SERS reporter labeled sequences,[9,10] and target DNA-induced distance change between Raman dye and substrate.[11,12] All these methods need to label the DNA probe prior to the assay procedure. Although the labeled DNA probe has been used for multiplex DNA detection,[13] some labeling processes are time-consuming and make the assay more complex. Therefore, label-free Raman techniques are attractive since they eliminate the complexity associated with preparation and attachment of appropriate labels.

Because of the poor SERS spectral reproducibility of DNA[14,15] and the same four bases in target DNA and probe sequences, the development of label-free SERS detection of DNA hybridization has been prevented. Fortunately, the single molecule sensitivity of SERS and the introduction of nanoparticles for improving the spectral reproducibility provide the possibility for label-free distinguishing of the single DNA base and detection of DNA.[15−23] Typically, by using 2-aminopurine to substitute the adenine base in probe sequence and Au shell-silica core nanoparticles to improve the reproducibility, a label-free SERS detection of DNA has been developed.[15] Recently, silver nanorod substrates have also been used to enhance the reproducibility for label-free SERS detection of nucleic acid hybridization by directly determining the composition ratios of four bases.[14] In addition, a heterogeneous SERS method has also been developed for label-free detection of DNA by direct electrostatic adsorption of positively charged silver nanoparticles and subsequent random incorporation of the SERS reporter.[24] This work presented a novel flexible label-free strategy for sensitive SERS detection of DNA by DNA-mediated silver nanoparticle growth.

DNA-mediated growth of metal nanoparticles has evoked substantial research activity in the generation of conductive nanowires and the construction of functional circuits.[25,26] Since DNA has a high affinity for metal cations, this technology provides a route to selectively form metal nanoparticles along with the DNA template. Moreover, these nanoparticles can be used as

Received: July 18, 2013
Accepted: October 31, 2013
Published: October 31, 2013

   dx.doi.org/10.1021/ac4032109 | *Anal. Chem.* 2013, 85, 11788−11793

Scheme 1. Schematic Illustration of Label-Free SERS Strategy for DNA Detection without (A) and with (B) HCR Amplification[a]

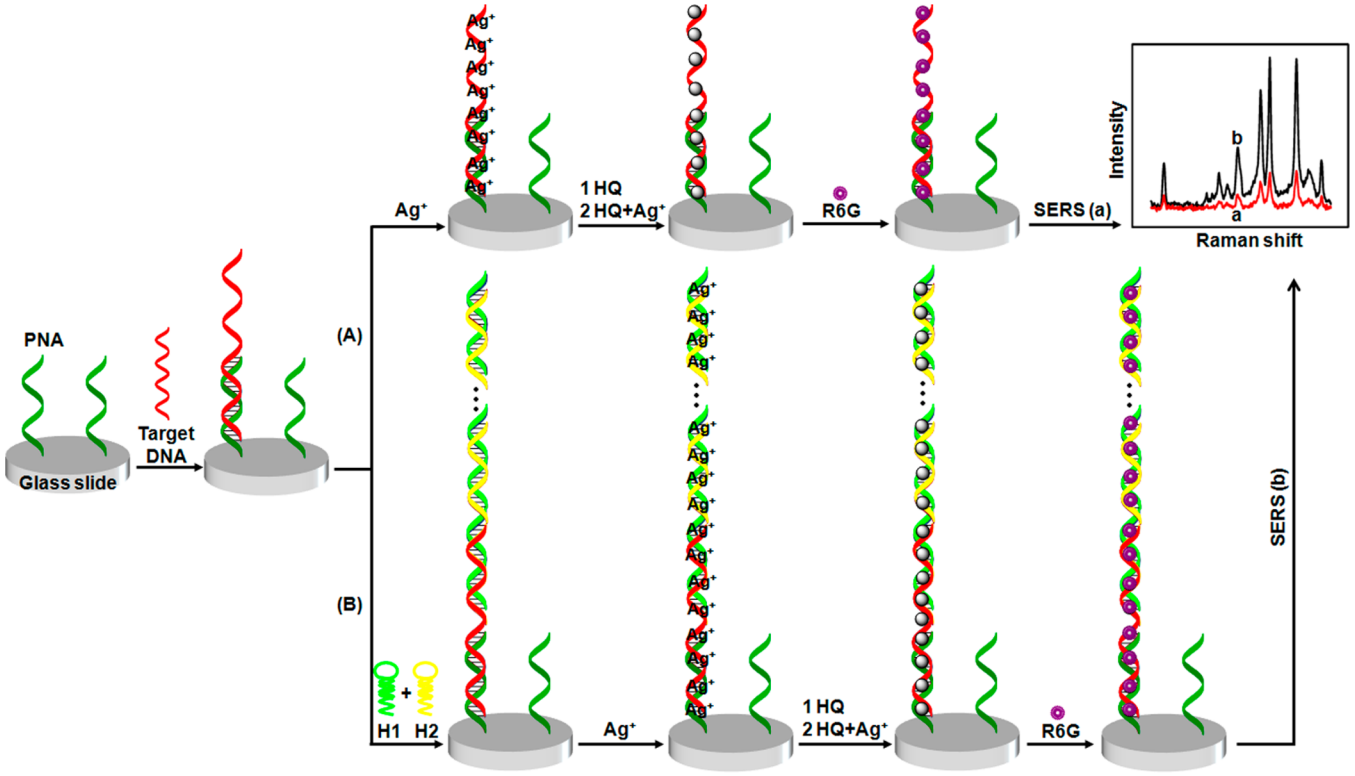

[a]HQ means hydroquinone.

nucleation sites for further deposition of metal nanoparticles,[27] such as silver,[28] gold,[29] palladium,[30] and platinum nanoparticles.[31] These DNA-based nanomaterials hold promise for application in nanodevices and biosensors.[32−36] In this work the target DNA was first captured by a peptide nucleic acid (PNA) modified glass slide, and the silver nanoparticles were then formed on the DNA skeleton by in situ chemical reduction of electrostatically absorbed Ag^+ cation and a followed silver deposition to act as a SERS active substrate for label-free SERS detection of DNA (Scheme 1A). The SERS reporter rhodamine 6G (R6G) could easily be absorbed by the silver nanoparticles.

The SERS signal generally depends on the amounts of absorbed reporter and the substrate. Thus the signal can be enhanced by extending the DNA chain using a molecular biological technique. The combination of rolling circle amplification (RCA) with Au nanoparticle and SERS reporter modified sequence has been used to amplify the SERS signal for detection of DNA down to 10 pM.[37] Here the DNA chain was extended through a simple hybridization chain reaction (HCR). The in situ silver nanoparticle deposition and growth simplified the SERS assay of target DNA (Scheme 1B). This method showed a detection limit of 3.4 pM and the ability of distinguishing single-base mismatch DNA without the need of both labeled sequence and enzymes. The DNA-mediated silver nanoparticle growth could be conveniently combined with other amplification techniques and thus provided an avenue for label-free sensitive Raman biosensing.

EXPERIMENTAL SECTION

Materials and Reagents. Sulfuric acid (70%), toluene, ammonium hydroxide (25%), $AgNO_3$, sodium citrate, citric acid, and hydrogen peroxide (30%) were obtained from Shanghai Reagent Co. (Shanghai, China). R6G, glycidoxypropyltrimethoxysilane (GPTMS) (98%), and hydroquinone were obtained from Sigma−Aldrich Inc. Phosphate buffer saline (PBS) was prepared by mixing the stock solutions of NaH_2PO_4 and Na_2HPO_4 (10 mM, pH 7.4). DNA hybridization buffer was phosphate-buffered saline (137 mM NaCl, 2.5 mM Mg^{2+}, 10 mM Na_2HPO_4, and 2.0 mM KH_2PO_4, pH 7.4). The citrate buffer was prepared by mixing the stock solutions of citric acid and sodium citrate (0.1 M, pH 3.5). Human serum samples were kindly provided by Jiangsu Cancer Hospital (Nanjing, China). A mixture containing equal volumes of human serum sample and DNA hybridization buffer was used for recovery testing. Ultrapure water obtained from a Millipore water purification system (18 MΩ, Milli-Q, Millipore) was used in all assays. PNA was purchased from Chengdu CP Biochem Co., Ltd. (Chengdu, China). DNA oligonucleotides were synthesized and purified by Takara Biotechnology Co., Ltd. (Dalian, China) and stored in DNA hybridization buffer. The sequences of these oligonucleotides are as follows:

PNA:	5′-NH_2-TATTAACTTTACTCC-3′
Target:	5′-TCAGCGGGGAGGAAGGGA GTAAAGTTAATA-3′
Hairpin probe 1 (H1):	5′-CTTCCTCCCCGCTGACAAA GTTCAGCGGGG-3′
Hairpin probe 2 (H2):	3′-GTTTCAAGTCGCCCCGAAG GAGGGGCGACT-5′
Single-base mismatch:	5′-TCAGCGGGGAGGAAGGGAG TAAAATTAATA-3′
Noncomplementary:	5′-GTGATCATACTTGGCAACT CGGTACCGCGC-3′
Capture probe:	5′-TATTAACTTTACTCC-3′

dx.doi.org/10.1021/ac4032109 | Anal. Chem. 2013, 85, 11788−11793

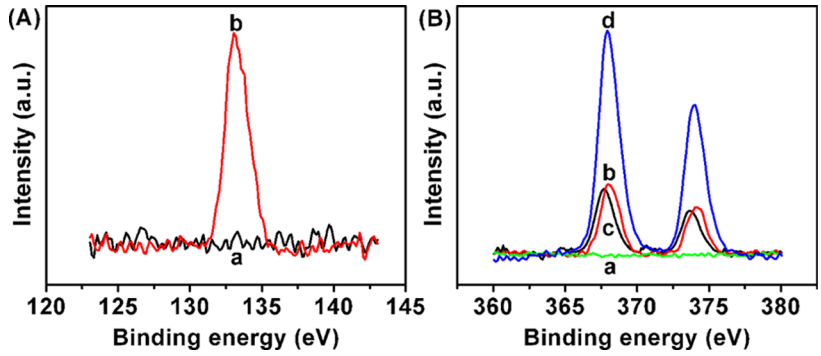

Figure 1. XPS spectra of (A) P2p for PNA (a) and target DNA–PNA duplex (b) and (B) Ag3d for (a) PNA after Ag^+ adsorption, (b) target DNA–PNA duplex after Ag^+ adsorption, (c) spectrum b after reduction of Ag^+, and (d) spectrum c after further growth of silver nanoparticles.

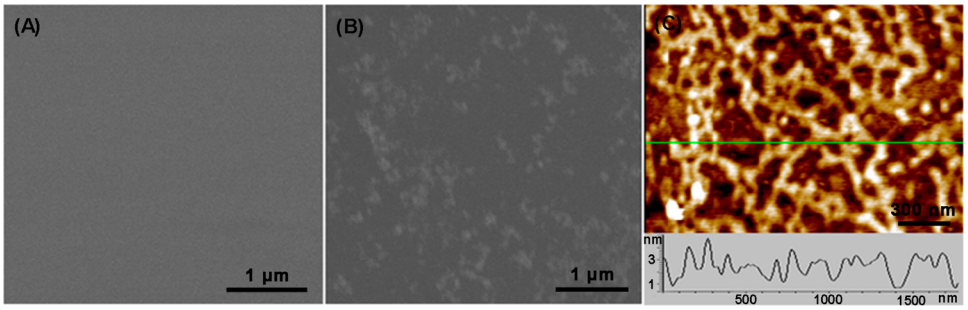

Figure 2. SEM images of (A) PNA and (B) target DNA–PNA duplex modified glass slides followed with silver reduction and growth, and (C) AFM height image of target DNA–PNA duplex modified glass slides followed with HCR, silver reduction, and growth.

DNA Hybridization. A glass substrate was first immersed in piranha solution (30% hydrogen peroxide and 70% sulfuric acid) for 12 h, washed thoroughly with water, and then dried under a stream of nitrogen. The obtained substrate was silylanized by dipping it in a toluene solution of 1% GPTMS overnight at room temperature.[38] Afterward, the substrate was washed thoroughly with toluene and ethanol to remove the physically absorbed GPTMS and dried under a stream of nitrogen. The immobilization of PNA on the silylanized substrate was performed by dropping 10 μL of PNA solution (1 μM) on the substrate and reacting at room temperature for 2 h.

After washing with 10 mmol L^{-1} PBS, the PNA modified substrate was soaked in 10 μL of target DNA solution at various concentrations for 1 h to capture the target DNA. After silver nanoparticle growth and R6G immobilization, the substrate was washed with water for obtaining the SERS signal. To amplify the SERS signal, the target DNA captured glass substrate was first incubated with a mixture of 10 μL of H1 (10 μM) and 10 μL of H2 (10 μM) for 2 h and then used to perform the silver nanoparticle growth and R6G immobilization.

Silver Deposition and R6G Immobilization. The DNA modified glass substrate was first incubated with 10 μL of $AgNO_3$ aqueous solution (0.1 M in ammonium hydroxide, pH 10.5) for 15 min to absorb Ag^+ ions on the DNA skeleton. After washing with 10 mmol L^{-1} PBS, 10 μL of hydroquinone solution (0.05 M in ammonium hydroxide, pH 10.5) was dropped on the substrate to reduce the absorbed Ag^+ ions for 15 min. The silver nanoparticles were then grown in 10 μL of citrate buffer (pH 3.5) containing hydroquinone (2.0 mM) and $AgNO_3$ (1.0 mM) for 8 min under low light conditions. After the substrate was washed with 10 mmol L^{-1} PBS, 10 μL of 0.05 mM R6G solution was dropped on the substrate for 2 h, which was then vigorously washed with 10 mmol L^{-1} PBS for Raman measurement.

Gel Electrophoresis. The 20% polyacrylamide gel electrophoresis (PAGE) analysis was carried out in 1× Tris-Borate-EDTA (pH 8.3) at a constant voltage of 100 V for about 2 h. After ethidium bromide staining, the gels were scanned using a Molecular Imager Gel Doc XR (Bio-Rad).

Apparatus. SERS measurements were performed using a Renishaw inVia-Reflex Raman microscope system (Renishaw, U.K.). An argon laser at 488 nm was used for excitation, and spectra were acquired using a 10× working objective lens on a sample. Scanning electron microscopic (SEM) images were obtained using a Hitachi S-4800 scanning electron microscope (Japan). Tapping mode atomic force microscopic (AFM) image was acquired under ambient conditions using an Agilent 5500 AFM/SPM system. X-ray photoelectron spectroscopic (XPS) measurements were performed using an ESCALAB 250 spectrometer (Thermo-VG Scientific) with an ultrahigh vacuum generator.

RESULTS AND DISCUSSION

Characterization of DNA-Mediated Silver Nanoparticle Growth. XPS was employed to confirm the assembly processes of the SERS system. The P2p XPS spectrum of PNA modified substrate did not show any detectable signal (Figure 1A, curve a). After the substrate captured target DNA, a P2p peak occurred at 133.1 eV, which corresponded to the phosphate group, indicating the presence of DNA (Figure 1A, curve b). The free anionic phosphate group of DNA backbone was expected to form the DNA–Ag^+ complex through electrostatic interaction. Thus the Ag3d XPS spectrum showed two new strong peaks at 374.1 and 368.1 eV compared to that in the absence of target DNA (Figure 1B, curves a and b), which correspond to Ag3d3/2

dx.doi.org/10.1021/ac4032109 | Anal. Chem. 2013, 85, 11788–11793

and Ag3d5/2, respectively. This result suggested that the PNA could not absorb Ag^+ due to their neutral backbone, while target DNA had high affinity for Ag^+. The reduction of Ag^+ by hydroquinone on the DNA skeleton led to slight position shift of Ag3d3/2 and Ag3d5/2 peaks to 373.8 and 367.8 eV (Figure 1B, curve c), respectively. After silver nanoparticle growth in an acidic solution of hydroquinone and $AgNO_3$, both the intensities of Ag3d3/2 and Ag3d5/2 peaks greatly increased (Figure 1B, curve d). These results indicated the formation and growth of silver nanoparticles on the DNA backbone, which provided a useful platform for subsequent SERS detection.

In the absence of target DNA, the PNA modified substrate could not absorb Ag^+. Thus the following silver reduction and growth processes did not produce any observable silver nanoparticles (Figure 2A). In contrast, after capturing target DNA, the formed DNA−PNA duplex produced abundant silver nanoparticles upon the reduction and growth processes (Figure 2B). The deposited silver nanoparticles were likely to take on an uneven agglomerated configuration due to the bending of DNA chain. AFM was also used to characterize the morphology of the silver nanoparticles decorated on DNA (Figure 2C). Because of the presence of predeposited silver nanoparticles, which only existed in the formed DNA−PNA duplex and acted as catalyst to accelerate the silver deposition process, the growth of silver nanoparticles was observed along the DNA skeleton. The associated height profile showed that the size of silver nanoparticles to be 2−3 nm. The silver nanoparticles could absorb the large amount of SERS reporter for sensitive SERS detection.

Feasibilty of Label-Free SERS Detection. The R6G molecule is stable under irradiating light and suitable for standard blue-to green excitation to produce a SERS signal.[39] In the absence of target DNA, Ag^+ adsorption, reduction, and growth and the followed R6G adsorption on the PNA modified substrate did not show any detectable Raman signal (Figure 3, curve a), indicating no silver nanoparticle was deposited or R6G was absorbed on the substrate surface. In the presence of target DNA, the grown silver nanoparticles did not also produce a Raman signal (Figure 3, curve b). Upon adsorption of R6G on the silver nanoparticles, a typical Raman vibration band of R6G appeared at 772, 1130, 1184, 1312, 1363, 1508, 1576, and 1651 cm^{-1} (Figure 3, curve c), which could be assigned to the carbon−hydrogen bend, ethylamine group wag, and xanthenes ring stretch of R6G,[32,40] respectively. The Raman signal enhanced by silver nanoparticles could be used for sensitive detection of DNA.

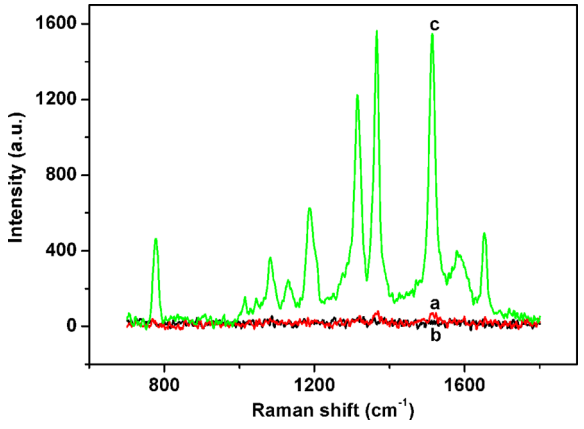

Figure 3. SERS spectra of (a) R6G absorbed on PNA modified glass slide after silver nanoparticle growth, (b) target DNA−PNA duplex modified glass slides after silver nanoparticle growth, and (c) spectrum b after further R6G adsorption.

Optimization of Detection Conditions. The SERS signal at 1508 cm^{-1} was selected for the detection of DNA. The intensity increased with the increasing silver growth time due to the local electromagnetic enhancement and the increasing amount of R6G absorbed on the silver nanoparticle surface.[41,42] The intensity reached a maximum value at 8 min. The longer deposition time led to a slight decrease of the overall SERS signal intensity since the larger particles absorbed less light but scattered more light through inelastic scattering.[43]

The amount of Raman dye absorbed on silver nanoparticles affected the SERS signal. With the increasing concentration of R6G from 0.01 to 0.05 mM for adsorption, the SERS intensity increased and then trended to a constant value (Figure 4B). Thus 0.05 mM was selected as the optimum concentration of R6G.

SERS Detection of Target DNA. Under optimal conditions, the SERS intensity increased dramatically with the increasing concentration of target DNA (Figure 5A), suggesting that DNA-mediated silver nanoparticles could be an effective SERS substrate for detection of DNA. The plot of SERS intensity vs the logarithm of target DNA concentration showed a good linearity in the range from 1.0×10^{-10} to 1.0×10^{-6} M (Figure 5B). The corresponding detection limit for the target was calculated to be 45 pM at 3σ.

To achieve higher detection sensitivity, HCR amplification was introduced to the detection protocol (Scheme 1B). HCR is an enzyme-free process where the hybridization event is triggered by target DNA as an initiator to produce oligonucleotide polymerization. It can achieve about 10-fold amplification at a constant temperature within a reaction time of 2 h.[44−46] After HCR, longer double-stranded DNA was generated for absorbing more Ag^+ cation and producing more silver nanoparticles to absorb more R6G, which led to a substantial increase in the corresponding SERS intensity. At the same target DNA concentrations of 0.1 μM and 10 nM, the SERS intensity with HCR (Figure 6A) were 3.5 and 4.1 times higher than those without HCR amplification (Figure 5A), respectively. The HCR process produced a linear range from 1.0×10^{-11} to 1.0×10^{-6} M for SERS detection of target DNA (Figure 6B). The limit of detection at 3σ was 3.4 pM, which was 13.2-fold lower than that without HCR amplification. The detection limit was also lower than 10 pM for a gold nanoparticle-on-nanowire SERS sensor[7] and a RCA-assistant SERS detection with Au nanoparticle and a SERS reporter modified sequence.[37]

Selectivity of SERS Detection Method. The selectivity of the proposed detection method was evaluated by using the complementary, single-base mismatch and noncomplementary DNA sequences at a concentration of 1.0 nM, respectively. As shown in Figure 7 for HCR-assistant SERS detection, the peak intensity at 1508 cm^{-1} for perfectly matched, single-base mismatch, and noncomplementary DNA was about 39.6, 8.5, and 1.8 times higher than the background signal, respectively, indicating that only the perfectly matched DNA triggered the HCR process efficiently. PAGE analysis was performed to evaluate the selectivity of the proposed method by using capture DNA with the same sequence to substitute PNA due to the neutral skeleton of PNA. As shown in the inset of Figure 7, the mixture of capture DNA and target DNA shows only one band due to the formation of dsDNA (lane c), while the mixture of capture DNA and single-base mismatched DNA at

dx.doi.org/10.1021/ac4032109 | Anal. Chem. 2013, 85, 11788−11793

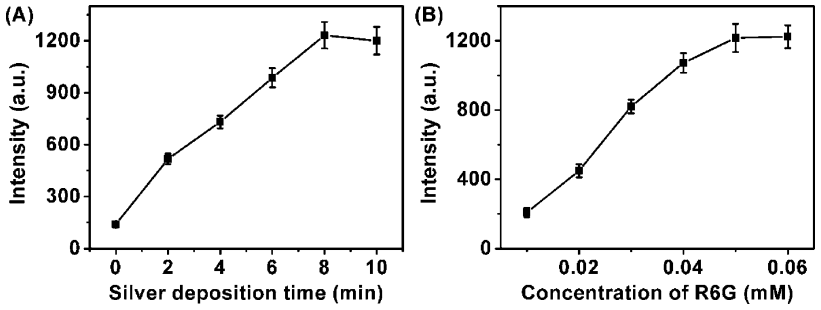

Figure 4. Dependence of SERS intensity on (A) silver nanoparticle growth time and (B) concentration of R6G.

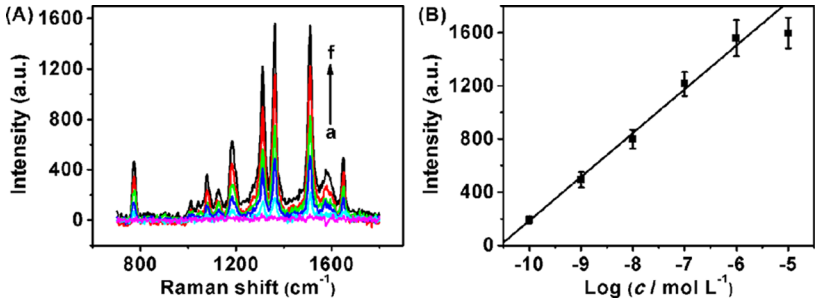

Figure 5. (A) SERS spectra for 10^{-11}, 10^{-10}, 10^{-9}, 10^{-8}, 10^{-7}, and 10^{-6} M target DNA (from a to f) without HCR amplification and (B) linear calibration of SERS intensity vs logarithm of DNA concentration.

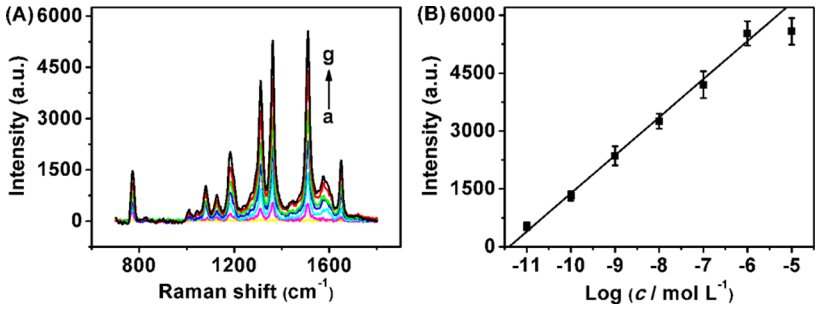

Figure 6. (A) SERS spectra for 10^{-12}, 10^{-11}, 10^{-10}, 10^{-9}, 10^{-8}, 10^{-7}, and 10^{-6} M target DNA (from a to g) with HCR amplification and (B) linear calibration of SERS intensity vs logarithm of DNA concentration.

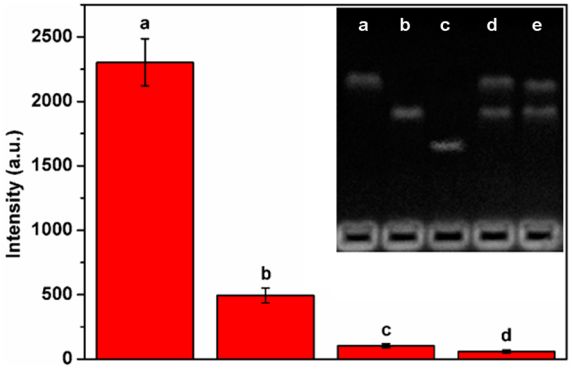

Figure 7. Histograms of SERS intensity for 1 nM of complementary (a), single-base mismatch (b), noncomplementary (c) sequences, and blank (d). Inset: PAGE analysis of 0.1 μM capture DNA (a), 0.1 μM target DNA (b), mixture of 0.1 μM capture DNA and target DNA (c), mixture of 0.1 μM capture DNA and single-base mismatched DNA (d), and mixture of 0.1 μM capture DNA and noncomplementary DNA (e).

the equal quantity showed two bands (lane d), which was the same as that for the mixture of capture DNA and non-complementary DNA (lane e), suggesting that the single-base mismatched and noncomplementary DNA could not hybridize with the capture probe. Therefore, this proposed method could effectively detect the target with high specificity.

Reproducibility for Target DNA Detection. The reproducibility of the suggested SERS detection method was examined by six repetitive measurements of 0.1 nM target DNA on a single substrate, which showed a relative standard deviation (RSD) of 2.4%. The RSD for six parallel DNA sensors fabricated on different substrates was 5.3%. These results indicated the satisfactory reproducibility for both DNA detection and DNA sensor fabrication.

Application in Real Sample. To test the generality of the proposed assay in the clinical sample, recovery testing was carried out by spiking target DNA solution into human serum. At the concentration of 10^{-10} and 10^{-8} M, the recoveries were 96.0 ± 1.7% and 94.1 ± 3.4% (n = 3), indicating that the proposed SERS strategy for DNA detection could be used in real sample analysis.

■ CONCLUSIONS

This study successfully constructed a label-free SERS detection method for DNA analysis by DNA-mediated silver nanoparticle

dx.doi.org/10.1021/ac4032109 | Anal. Chem. 2013, 85, 11788−11793

growth on a PNA modified glass slide. The anionic phosphate group of DNA was indentified to have high affinity for Ag^+ cation. The Ag^+ cation absorbed on the DNA skeleton could be chemically reduced to form silver nanoparticles, which were then further grown with a silver enhancement step for absorption of R6G as a Raman reporter. By combining with HCR, the DNA skeleton could be extended to deposit more silver nanoparticles for absorbing more R6G, leading to significantly amplified SERS signal and a 13.2-fold lower limit detection. The proposed label-free SERS strategy showed high selectivity against a single-base mismatch sequence due to the intrinsic functions of HCR. The DNA-mediated silver nanoparticle growth offers the versatile platform for label-free SERS detection of DNA in a cost-effective manner and has a promising application in clinical diagnosis.

AUTHOR INFORMATION

Corresponding Author

*Phone/fax: +86-25-83593593. E-mail: hxju@nju.edu.cn.

Notes

The authors declare no competing financial interest.

ACKNOWLEDGMENTS

This work was financially supported by the National Basic Research Program of China (Grant 2010CB732400) and the National Natural Science Foundation of China (Grants 21135002, 21121091).

REFERENCES

(1) Johnson, R. P.; Richardson, J. A.; Brown, T.; Bartlett, P. N. *J. Am. Chem. Soc.* **2012**, *134*, 14099−14107.
(2) Li, J. F.; Huang, Y. F.; Ding, Y.; Yang, Z. L.; Li, S. B.; Zhou, X. S.; Fan, F. R.; Zhang, W.; Zhou, Z. Y.; Wu, D. Y.; Ren, B.; Wang, Z. L.; Tian, Z. Q. *Nature* **2010**, *464*, 392−395.
(3) Lierop, D. V.; Larmour, I. A.; Faulds, K.; Graham, D. *Anal. Chem.* **2013**, *85*, 1408−1414.
(4) He, Y.; Su, S.; Xu, T. T.; Zhong, Y. L.; Zapien, J. A.; Li, J.; Fan, C. H.; Lee, S. T. *Nano Today* **2011**, *6*, 122−130.
(5) Lim, D. K.; Jeon, K. S.; Kim, H. M.; Nam, J. M.; Suh, Y. D. *Nat. Mater.* **2010**, *9*, 60−67.
(6) Cao, Y. C.; Jin, R.; Mirkin, C. A. *Science* **2002**, *297*, 1536−1540.
(7) Kang, T.; Yoo, S. M.; Yoon, I.; Lee, S. Y.; Kim, B. *Nano Lett.* **2010**, *10*, 1189−1193.
(8) Zhang, H.; Harpster, M. H.; Park, H. J.; Johnson, P. A. *Anal. Chem.* **2011**, *83*, 254−260.
(9) Graham, D.; Thompson, D. G.; Smith, W. E.; Faulds, K. *Nat. Nanotechnol.* **2008**, *3*, 548−551.
(10) Wabuyele, M. B.; Vo-Dinh, T. *Anal. Chem.* **2005**, *77*, 7810−7815.
(11) Ngo, H. T.; Wang, H. N.; Fales, A. M.; Vo-Dinh, T. *Anal. Chem.* **2013**, *85*, 6378−6383.
(12) Qian, X.; Zhou, X.; Nie, S. M. *J. Am. Chem. Soc.* **2008**, *130*, 14934−14935.
(13) Sun, L.; Yu, C.; Irudayaraj, J. *Anal. Chem.* **2007**, *79*, 3981−3988.
(14) Abell, J. L.; Garren, J. M.; Driskell, J. D.; Tripp, R. A.; Zhao, Y. P. *J. Am. Chem. Soc.* **2012**, *134*, 12889−12892.
(15) Barhoumi, A.; Halas, N. J. *J. Am. Chem. Soc.* **2010**, *132*, 12792−12793.
(16) Papadopoulou, E.; Bell, S. E. J. *Angew. Chem., Int. Ed.* **2011**, *50*, 9058−9061.
(17) Domke, K. F.; Zhang, D.; Pettinger, B. *J. Am. Chem. Soc.* **2007**, *129*, 6708−6709.
(18) Barhoumi, A.; Zhang, D. M.; Tam, F.; Halas, N. J. *J. Am. Chem. Soc.* **2008**, *130*, 5523−5529.
(19) Papadopoulou, E.; Bel, S. E. J. *Chem. Commun.* **2011**, *47*, 10966−10968.
(20) Green, M.; Liu, F. M.; Cohen, L.; Kollensperger, P.; Cass, T. *Faraday Discuss.* **2006**, *132*, 269−280.
(21) Driskell, J. D.; Seto, A. G.; Jones, L. P.; Jokela, S.; Dluhy, R. A.; Zhao, Y. P.; Tripp, R. A. *Biosens. Bioelectron.* **2008**, *24*, 917−922.
(22) Shanmukh, S.; Jones, L.; Driskell, J.; Zhao, Y.; Dluhy, R.; Tripp, R. A. *Nano Lett.* **2006**, *6*, 2630−2636.
(23) Marotta, N. E.; Beavers, K. R.; Bottomley, L. A. *Anal. Chem.* **2013**, *85*, 1440−1446.
(24) Fabris, L.; Dante, M.; Braun, G.; Lee, S. J.; Reich, N. O.; Moskovits, M.; Nguyen, T. Q.; Bazan, G. C. *J. Am. Chem. Soc.* **2007**, *129*, 6086−6087.
(25) Braun, E.; Eichen, Y.; Sivan, U.; Ben-Yoseph, G. *Nature* **1998**, *391*, 775−778.
(26) Yan, H.; Park, S. H.; Finkelstein, G.; Reif, J. H.; LaBean, T. H. *Science* **2003**, *301*, 1882−1884.
(27) Keren, K.; Berman, R. S.; Braun, E. *Nano Lett.* **2004**, *4*, 323−326.
(28) Liu, D.; Park, S. H.; Reif, J. H.; LaBean, T. H. *Proc. Natl. Acad. Sci. U.S.A.* **2004**, *101*, 717−722.
(29) Ongaro, A.; Griffin, F.; Beeeher, P.; Nagle, L.; Iacopino, D.; Quinn, A.; Redmond, G.; Fitzmaurice, D. *Chem. Mater.* **2005**, *17*, 1959−1964.
(30) Liu, H. P.; Chen, Y.; He, Y.; Ribbe, A. E.; Mao, C. D. *Angew. Chem., Int. Ed.* **2006**, *45*, 1942−1945.
(31) Ford, W. E.; Harnack, O.; Yasuda, A.; Wessels, J. M. *Adv. Mater.* **2001**, *13*, 1793−1797.
(32) Shang, L.; Wang, Y. L.; Huang, L. J.; Dong, S. J. *Langmuir* **2007**, *23*, 7738−7744.
(33) Becerril, H. A.; Stoltenberg, R. M.; Wheeler, D. R.; Davis, R. C.; Harb, J. N.; Woolley, A. T. *J. Am. Chem. Soc.* **2005**, *127*, 2828−2829.
(34) Roy, S.; Chen, X. J.; Li, M. H.; Peng, Y. F.; Anariba, F.; Gao, Z. Q. *J. Am. Chem. Soc.* **2009**, *131*, 12211−12217.
(35) Keren, K.; Krueger, M.; Gilad, R.; Ben-Yoseph, G.; Sivan, U.; Braun, E. *Science* **2002**, *297*, 72−75.
(36) Wang, J.; Rincon, O.; Polsky, R.; Dominguez, E. *Electrochem. Commun.* **2003**, *5*, 83−86.
(37) Hu, J.; Zhang, C. Y. *Anal. Chem.* **2010**, *82*, 8991−8997.
(38) Ruan, C. M.; Yang, L. J.; Li, Y. B. *Anal. Chem.* **2002**, *74*, 4814−4820.
(39) Ishikawa, M.; Maruyama, Y.; Ye, J. Y.; Futamata, M. *J. Lumin.* **2002**, *98*, 81−89.
(40) Hildebrandt, P.; Stockburger, M. *J. Phys. Chem.* **1984**, *88*, 5935−5944.
(41) Kelly, K. L.; Coronado, E.; Zhao, L. L.; Schatz, G. C. *J. Phys. Chem. B* **2003**, *107*, 668−677.
(42) Pustovit, V.; Shahbazyan, T. *Microelectron. J.* **2005**, *36*, 559−563.
(43) Stamplecoskie, K. G.; Scaiano, J. C. *J. Phys. Chem. C* **2011**, *115*, 1403−1409.
(44) Liu, S. F.; Wang, Y.; Ming, J. J.; Lin, Y.; Cheng, C. B.; Li, F. *Biosens. Bioelectron.* **2013**, *49*, 472−477.
(45) Zhuang, J. Y.; Fu, L. B.; Xu, M. D.; Yang, H. H.; Chen, G. N.; Tang, D. P. *Anal. Chim. Acta* **2013**, *78*, 17−23.
(46) Chen, Y.; Xu, J.; Su, J.; Xiang, Y.; Yuan, R.; Chai, Y. Q. *Anal. Chem.* **2012**, *84*, 7750−7755.